As S/N decreases below unity, detection of curvature quickly becomes impossible.

For the data points plotted in Figure 1, $x = pK_a$ and $f(x) = \log k_r$. The latter was calculated from eq 7, using the parameters resulting from the least-squares fit for mechanism 2. Values of S/N computed in this way for the five plots shown in Figure 1 range from 0.6 to 0.7, the mean S/N being 0.66. This is well below unity. One may conclude, therefore, that the predicted curvature of the plots is too gentle to be detected.

A second fitting comment concerns solvation effects, or rather the number of adjustable parameters to be used. When the formation of a reactive encounter complex from the reagents needs to be treated as a separate prior equilibrium, Marcus[4] and others[6,8d,9,10b] have suggested modifications of the basic theory which would recast eq 7 in the form:

$$\Delta G^{\ddagger} = \gamma^{\circ} + \tfrac{1}{2}\Delta G^{\circ} + (\Delta G^{\circ})^2/16\mu^{\circ} - (\Delta G')^2/16\mu' \qquad (27)$$

There are now three adjustable parameters: γ°, μ°, and μ'. The original γ in eq 7 has been replaced by γ° and μ°: γ° gathers up all effects on reactivity that remain constant in the reaction series, while μ° gathers up all effects that vary as $(\Delta G^{\circ})^2$. Their values are different if certain physical effects, including solvation effects in the formation of reactive encounter complexes, become important. μ' corresponds to μ in eq 7.

The fit of the three-parameter eq 27 represents an improvement over that of eq 7. Using the same 25 data sets as before (Table II), least-squares results are: $\gamma^{\circ} = 12.66 \pm 0.2$ kcal; $\mu^{\circ} = 21.8 \pm 2.8$ kcal; $\mu' = 3.66 \pm 0.8$ kcal. σ(fit) = 0.137 kcal, which compares favorably with that of eq 7, 0.188 kcal, and is consistent with the 0.14-kcal experimental error of $\Delta G_+^{\ddagger}$. Because the formal change from (7) to (27) has a physical basis, the improvement of fit is not trivially due merely to the introduction of an additional parameter.

Despite this good result, I prefer eq 7 for the investigation of reaction mechanism. The physical basis of eq 7 is of broad scope, and although there are soft spots, the inherent approximations are understood. Using eq 7, transition-state coordinates can be simply deduced. Assuming that eq 2 represents the dominant mechanism, the fit of eq 7 is really quite good, and one ought not add to the pitfalls in deducing reaction mechanism by needlessly increasing the number of adjustable parameters.

Registry No. CH_2O, 50-00-0; CH_3CH_2OH, 64-17-5; $CH_3OCH_2CH_2OH$, 109-86-4; $ClCH_2CH_2OH$, 107-07-3; Cl_2CHCH_2OH, 598-38-9; CF_3CH_2OH, 75-89-8; CH_3COO^-, 71-50-1; $ClCH_2CH_2COO^-$, 5102-76-1; $CH_3OCH_2COO^-$, 20758-58-1; $ClCH_2COO^-$, 14526-03-5; $NCCH_2COO^-$, 23297-32-7.

Reaction Mechanism from Structure–Energy Relations. 2. Acid-Catalyzed Addition of Alcohols to Formaldehyde

Ernest Grunwald

Contribution from the Chemistry Department, Brandeis University, Waltham, Massachusetts 02254. *Received November 16, 1984*

Abstract: Previous theory of structure–energy relations is extended to mechanisms with three concerted reaction events. Data for 25 reactions (five alcohols, five acid catalysts) are examined on the basis of four different mechanisms. Only one of the mechanisms fits well. It involves concerted C···O bond formation, proton donation by the acid catalyst, and proton acceptance by a water molecule, according to $H_2O + HOCH_2R + H_2C{=}O + HOOCCH_2R' \rightarrow H_2OH^+ + RCH_2OCH_2OH + {}^-OOCCH_2R'$. The fit for this mechanism is decisively good in three practically independent tests. The contrast between the present mechanism and that which fits the base-catalyzed reaction (which does not involve HOH as a reagent) can be explained as due to peculiarities of relative acid–base properties of RCH_2OCH_2OH and H_2O. No inconsistency appears with other data. Transition-state coordinates for the acid-catalyzed reaction are tabulated. Progress of C···O bond formation, though variable within the reaction series, is well ahead of that of the proton transfers. Further analysis of the theoretical free-energy surfaces indicates that disparity of progress of the concerted reaction events reaches a maximum at the transition state.

This paper continues the use of structure–energy relations for deducing the mechanism of the addition of alcohols to formaldehyde. The preceding paper[1] (hereafter called part 1) examines the mechanism of general base catalysis, using a theory of reactivity[2] which applies when there is disparity of progress of two concerted reaction events. This theory, which develops Marcus rate–equilibrium theory[3] so as to quantify the use of More O'Ferrall diagrams,[4] predicts diagnostically different structure–energy relations for different reaction mechanisms. In the case of base catalysis, only one of the suggested mechanisms fits the data, and this mechanism agrees with that indicated by other methods.[1,5,6]

I shall now examine the mechanism of general acid catalysis. The specific reaction series is shown symbolically in eq 1, where R and R′ are variable substituents.

$$R'CH_2COOH + RCH_2OH + H_2C{=}O \underset{{}^{a}k_r}{\overset{{}^{a}k_f}{\rightleftharpoons}} RCH_2OCH_2OH + R'CH_2COOH \qquad (1)$$

I shall use a 5 × 5 matrix of data: five primary alcohols and five carboxylic acid catalysts, as reported by Funderburk, Aldwin, and Jencks (FAJ).[5] The experimental rate constants ${}^{a}k_r$ apply to the *reverse* reaction in eq 1, which was caused to go to completion by trapping the formaldehyde.

Brønsted plots of $\log {}^{a}k_r$ vs. pK_a of the acid catalyst are shown in Figure 1. Plots of $\log {}^{a}k_r$ vs. pK_a of the alcohol are shown in Figure 2. These figures also show best-fitting straight lines obtained by least squares. Most of the lines reproduce the data adequately. However, as pointed out before,[1] there is no statistical necessity for the real relationships to be straight lines. They may be gentle curves.

(1) Grunwald, E. *J. Am. Chem. Soc.*, preceding paper in this issue.
(2) Grunwald, E. *J. Am. Chem. Soc.* **1985**, *107*, 125.
(3) Marcus, R. A. *J. Phys. Chem.* **1968**, *72*, 891.
(4) More O'Ferrall, R. A. *J. Chem. Soc. B* **1970**, 274.
(5) Funderburk, L. H.; Aldwin, L.; Jencks, W. P. *J. Am. Chem. Soc.* **1978**, *100*, 5444.
(6) Palmer, J. L.; Jencks, W. P. *J. Am. Chem. Soc.* **1980**, *102*, 6472.

0002-7863/85/1507-4715$01.50/0

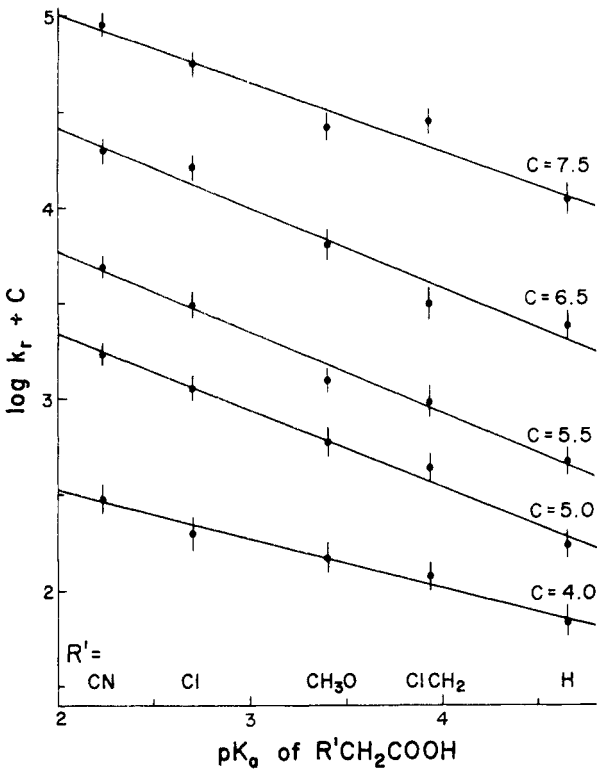

Figure 1. Brønsted plots for acid-catalyzed cleavage of RCH_2OCH_2OH in water vs. pK_a of the acid catalyst. (Top to bottom) *C*, R substituent, slope of straight line: 7.5, CF_3, −0.352; 6.5, Cl_2CH, −0.421; 5.5, $ClCH_2$, −0.422; 5.0, CH_3OCH_2, −0.400; 4.0, CH_3, −0.251, (data from ref 5).

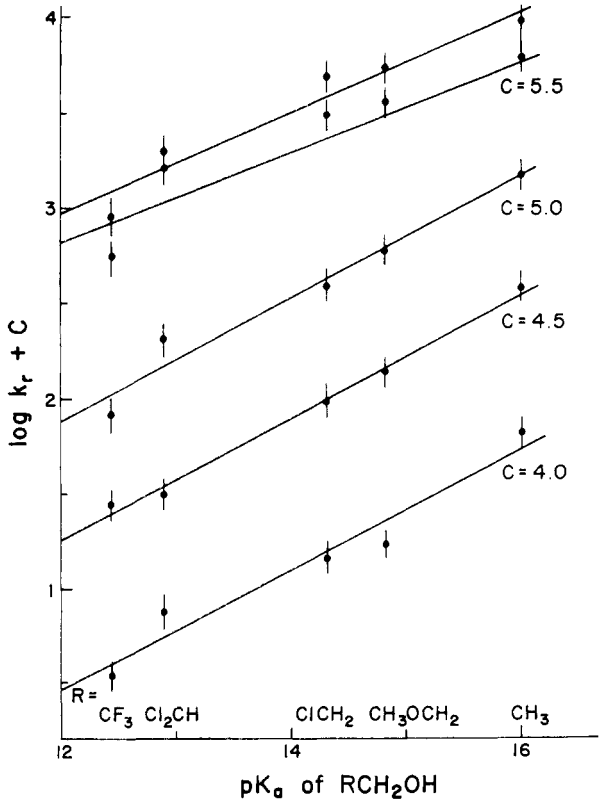

Figure 2. Logarithmic plot of rate constant for acid-catalyzed cleavage of RCH_2OCH_2OH in water vs. pK_a of the alcohol produced. (Top to bottom) Acid R′ substituent, slope of straight line: CN, 0.269; Cl, 0.260; CH_3O, 0.319; $ClCH_2$, 0.320; H, 0.319 (data from ref 5).

It will turn out that suggested reaction mechanisms involving two concerted reaction events do not fit the data well. I shall therefore extend the diagnostic theory to mechanisms involving three concerted reaction events. When energy depends on three

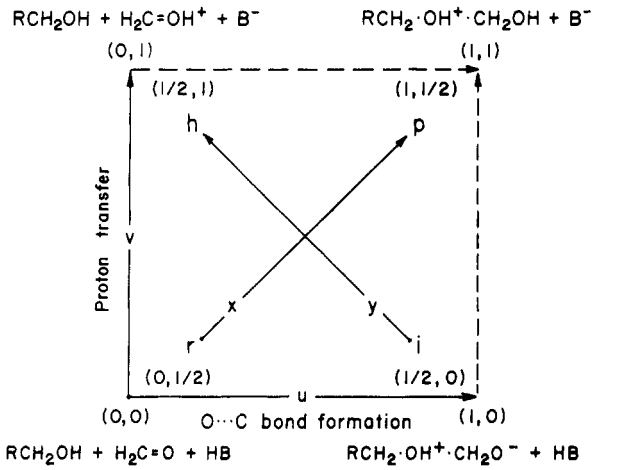

Figure 3. Progress square with corner species for the rate-determining step (2a) of the acid-catalyzed mechanism 2.

progress variables, the full coordinate space becomes four-dimensional, and graphical representation by More O'Ferrall diagrams becomes inconvenient. On the other hand, analytical representation by the theoretical equations remains convenient.

Mechanisms with Two Progress Variables. FAJ[5] considered the two kinetically equivalent mechanisms 2 and 3. They favor mechanism 2.

$$RCH_2OH + H_2C{=}O + HB \underset{k_-}{\overset{k_+}{\rightleftharpoons}} RCH_2{\cdot}OH^+{\cdot}CH_2OH + B^- \quad (2a)$$

$$RCH_2{\cdot}OH^+{\cdot}CH_2OH + B^- \overset{\text{fast}}{\rightleftharpoons} RCH_2OCH_2OH + HB \quad (2b)$$

$$CH_2{=}O + HB \overset{\text{fast}}{\rightleftharpoons} CH_2{=}OH^+ + B^- \quad (3a)$$

$$B^- + HOCH_2R + CH_2{=}OH^+ \underset{k_-'}{\overset{k_+'}{\rightleftharpoons}} HB + RCH_2OCH_2OH \quad (3b)$$

The concerted reaction events in both slow steps 2a and 3b are proton transfer and C···O bond formation. For step 2a this is shown by a More O'Ferrall diagram in Figure 3. The process i → h in that figure is the disparity reaction associated with (2a) and is shown explicitly in eq disp. 2a. The disparity reaction for step 3b is shown in eq disp. 3b.

$$RCH_2{\cdot}OH^+{\cdot}CH_2O^- + HB \rightarrow RCH_2OH + H_2C{=}OH^+ + B^- \quad \text{(disp. 2a)}$$

$$B^- + RCH_2{\cdot}OH^+{\cdot}CH_2OH \rightarrow HB + RCH_2O^- + CH_2{=}OH^+ \quad \text{(disp. 3b)}$$

The theoretical structure–energy relation for two progress variables is eq 7 of part 1.[1] Let ${}^a k_r = (k_B T/h) \exp(-\Delta G_r^{\ddagger}/RT)$. The required free-energy quantities then are related to auxiliary free-energy quantities defined and tabulated in part 1 (eq 10–16 and Table I) as follows.[1] For step 2a:

$$\Delta G^\circ = \Delta G^{\text{hemi}} - \Delta G^{\text{IH}} + \Delta G^{\text{HB}} \quad (2c)$$

$$\Delta G' = -\Delta G^{\text{hemi}} - \Delta G^{\text{K}} - \Delta G^{\text{Z}} + \Delta G^{\text{HB}} \quad (2d)$$

$$\Delta G_+^{\ddagger} = \Delta G_r^{\ddagger} + \Delta G^{\text{hemi}} \quad (2e)$$

For step 3b:

$$\Delta G^\circ = \Delta G^{\text{hemi}} + \Delta G^{\text{K}} - \Delta G^{\text{HB}} \quad (3c)$$

$$\Delta G' = -\Delta G^{\text{HB}} - \Delta G^{\text{K}} + \Delta G^{\text{HOR}} - \Delta G^{\text{hemi}} + \Delta G^{\text{IH}} \quad (3d)$$

$$\Delta G_+^{\ddagger} = \Delta G_r^{\ddagger} + \Delta G^{\text{hemi}} + \Delta G^{\text{K}} - \Delta G^{\text{HB}} \quad (3e)$$

For both mechanisms the fit to eq 7 of part 1 is poor; σ(fit) is at least twice σ(data). For mechanism 2, σ(fit) = 0.56 kcal and σ(data) = 0.28 kcal. For mechanism 3, σ(fit) = 0.46 kcal and σ(data) = 0.21 kcal. Apparently neither mechanism represents

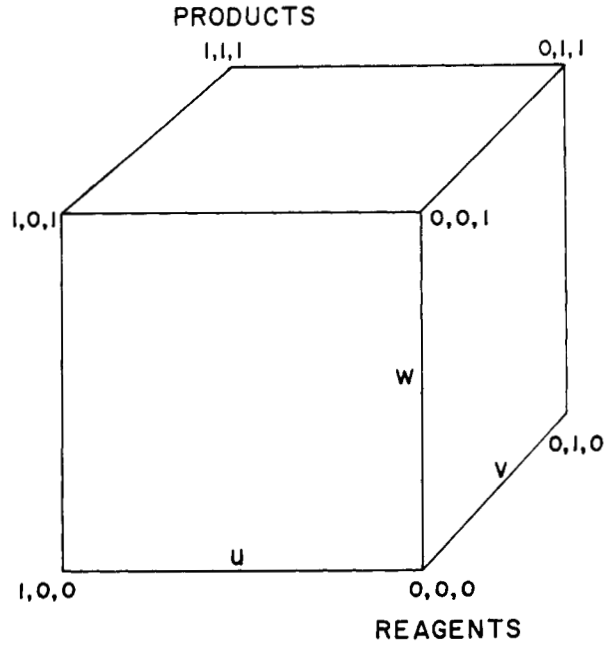

Figure 4. Progress cube in (u,v,w) coordinates with labels for corner species.

the dominant process of the acid-catalyzed reaction.

I believe these negative results are significant, for two reasons. First, the method used here is identical with that which fits the complicated facts for the otherwise identical base-catalyzed reaction. Second, from a chemical point of view, the product in (2a), $RCH_2{\cdot}OH^+{\cdot}CH_2OH$, is a stronger acid than H_3O^+. Thus, if the process shown in (2a) were coupled to proton transfer to solvent water as in (4), the free energy of activation would be reduced.

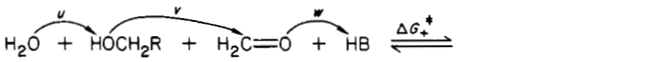

$$H_3O^+ + RCH_2OCH_2OH + B^- \quad (4)$$

By contrast, the species $RCH_2OCH_2O^-$ produced in the base-catalyzed mechanism is a weaker base than OH^-, and coupling of its formation to proton transfer from solvent water is less likely. (Data are given in Table I of part 1.)[1]

Since reaction 4 involves three concerted reaction events (labeled u, v, and w), I shall first present the basic physical theory, and then apply it to show that the mechanism suggested in (4) fits the data well.

Three Progress Variables. The progress diagram, Figure 4, is now a unit cube. The three progress variables are denoted by u, v, and w. The point representing the reagents is (0,0,0); that representing the products is (1,1,1). The other corner points represent the six intermediates that can be formed when the three reaction events occur stepwise rather than simultaneously.

In order to apply Marcus rate–equilibrium theory, it is necessary to rotate, translate, and renormalize this coordinate system, because one of the new coordinate axes must join reagents directly to products and thus measure mean progress of the reaction events.[2] The other two coordinates may then be chosen so as to measure disparity of progress of the reaction events. If possible, their end points should represent states of known or predictable energy, i.e., be corner points of the (u,v,w) cube.

I find it convenient to rotate the (u,v,w) system by the following values of the Euler angles:[7] $\zeta = \cos^{-1}(1/\sqrt{3}) = 54°\ 44'$; $\theta = 45°$; $\phi = 0°$. Renormalization and translation of the origin so that the new axes intersect at $^1/_2,^1/_2,^1/_2$ then leads to the following new coordinates:

$$x = (u + v + w)/3 \quad (5a)$$

$$y_u = \tfrac{1}{2} + \tfrac{1}{2}(-u + [v + w]/2) \quad (5b)$$

$$s_u = \tfrac{1}{2} + \tfrac{1}{2}(-v + w) = \tfrac{1}{2} + \tfrac{1}{2}([-u + w] - [-u + v]) \quad (5c)$$

According to (5a), x measures mean progress. According to (5b), $y_u - {}^1/_2$ measures the disparity, relative to u, of the mean progress of v and w. According to (5c), $s_u - {}^1/_2$ measures the *difference* between the disparities of progress, relative to u, of w and v.

In eq 5, u is the pivot variable relative to which disparities of progress are measured. By appropriate rotations, other sets of variables, (6) and (7), can be obtained in which v are w are pivot variables.

$$x = (u + v + w)/3 \quad (6a, 7a)$$

$$y_v = \tfrac{1}{2} + \tfrac{1}{2}(-v + [u + w]/2) \quad (6b)$$

$$s_v = \tfrac{1}{2} + \tfrac{1}{2}(-u + w) \quad (6c)$$

$$y_w = \tfrac{1}{2} + \tfrac{1}{2}(-w + [u + v]/2) \quad (7b)$$

$$s_w = \tfrac{1}{2} + \tfrac{1}{2}(-u + v) \quad (7c)$$

Returning to coordinates 5 with pivot variable u, the free energy G is given by eq 8, which is a fairly obvious extension of previous theory[2] from two to three progress variables. Aspects of its derivation will be considered in a later section.

$$G = c + 4\gamma x(1 - x) + \Delta G°x - 4\mu_u y_u(1 - y_u) + \Delta G'_u y_u - 4\mu'_u s_u(1 - s_u) + \Delta G''_u s_u \quad (8)$$

As before, c is a constant depending on the zero point of the free-energy scale. The intrinsic barrier γ and the intrinsic wells μ_u and μ'_u are characteristic constants for the reaction series or family.

$\Delta G°$, $\Delta G'_u$, and $\Delta G''_u$ denote the free-energy changes for full displacements along x, y_u, and s_u, respectively. They are specific for each reaction. To define the processes to which they apply, I shall let brackets denote coordinates in the $[x,y_u,s_u]$ system and parentheses in the (u,v,w) system. The reagents are located at $[0,^1/_2,^1/_2]$ and the products at $[1,^1/_2,^1/_2]$. These points correspond to (0,0,0) and (1,1,1), respectively, in (u,v,w). Full displacement along the x axis from reagents to products thus defines $\Delta G°$ as the free-energy change for the process, (0,0,0) → (1,1,1).

The end points of the y_u axis are at $[^1/_2,0,^1/_2]$ and $[^1/_2,1,^1/_2]$ in $[x,y_u,s_u]$, and correspond to (1,0,0) and (0,1,1) in (u,v,w). Full displacement along the y_u axis thus defines $\Delta G'_u$ as the free-energy change for the process (1,0,0) → (0,1,1).

The end points of the s_u axis are $[^1/_2,^1/_2,0]$ and $[^1/_2,^1/_2,1]$ in $[x,y_u,s_u]$, and correspond to $(^1/_2,1,0)$ and $(^1/_2,0,1)$ in (u,v,w). In contrast to the end points of x and y_u, which correspond to corner species in (u,v,w) (see Figure 4) and whose free energies thus are known or predictable, the end points of s_u are *not* corner species. They lie at the corners of a square plane normal to the u axis at $u = {}^1/_2$. Their molecular configurations and hence their free energies are less predictable than those of corner species. Fortunately, within the framework of the present theory, one can relate their free energies to the free energy of corner species in (u,v,w). One predicts, by straightforward substitution of (5) in (8), that for any change $(u,1,0) \rightarrow (u,0,1)$, $0 \le u \le 1$, ΔG is constant and simply equal to $\Delta G''_u$, independent of u. Thus, if eq 8 is at least approximately valid, one may simulate the displacement $(^1/_2,1,0) \rightarrow (^1/_2,0,1)$ along s_u by the process shown in (9), involves corner species.

$$\tfrac{1}{2}(0,1,0) + \tfrac{1}{2}(1,1,0) \rightarrow \tfrac{1}{2}(0,0,1) + \tfrac{1}{2}(1,0,1) \quad \Delta G''_u \quad (9)$$

When v or w are pivot variables, equations and processes for the free-energy quantities are obtained analogously. Let p denote the chosen pivot variable, which may be u, v, or w. Then G is expressed by eq 10, where the intrinsic constants and specific

$$G = c + 4\gamma x(1 - x) + \Delta G°x - 4\mu_p y_p(1 - y_p) + \Delta G'_p y_p - 4\mu'_p s_p(1 - s_p) + \Delta G''_p s_p \quad (10)$$

free-energy changes are like those in (8) but depend on the choice of pivot variable. Practical equations and related processes are given in Table I.

(7) See, for example, Goldstein, H. "Classical Mechanics"; Addison-Wesley: Reading, MA, 1950.

Table I. Equations and Processes for Three Progress Variables

pivot	variable [process in (u,v,w)]
u,v,w	ΔG° [(0,0,0) → (1,1,1)]
u	$\Delta G'_u$ [(1,0,0) → (0,1,1)]
	$\Delta G''_u = {}^1/_2(\Delta G'_v - \Delta G'_w)$
	[${}^1/_2$(0,1,0) + ${}^1/_2$(1,1,0) → ${}^1/_2$(1,0,1) + ${}^1/_2$(0,0,1)]
	$u^* = x^* - 4y_u^*/3 + 2/3$
	$v^* = x^* + 2y_u^*/3 - s_u^* + 1/6$
	$w^* = x^* + 2y_u^*/3 + s_u^* - 5/6$
v	$\Delta G'_v$ [(0,1,0) → (1,0,1)]
	$\Delta G''_v = {}^1/_2(\Delta G'_u - \Delta G'_w)$
	${}^1/_2$(1,1,0) + ${}^1/_2$(1,0,0) → ${}^1/_2$(0,1,1) + ${}^1/_2$(0,0,1)]
	$u^* = x^* + 2y_v^*/3 - s_v^* + 1/6$
	$v^* = x^* - 4y_v^*/3 + 2/3$
	$w^* = x^* + 2y_v^*/3 + s_v^* - 5/6$
w	$\Delta G'_w$ [(0,0,1) → (1,1,0)]
	$\Delta G''_w = {}^1/_2(\Delta G'_u - \Delta G'_v)$
	[${}^1/_2$(1,0,0) + ${}^1/_2$(1,0,1) → ${}^1/_2$(0,1,1) + ${}^1/_2$(0,1,0)]
	$u^* = x^* + 2y_w^*/3 - s_w^* + 1/6$
	$v^* = x^* + 2y_w^*/3 + s_w^* - 5/6$
	$w^* = x^* - 4y_w^*/3 + 2/3$

Table II. Test[a] of Mechanism 4

$\Delta G_+^* = \Delta G_r^* + \Delta H^{hemi} + RT \ln [HOH]$
$\Delta G^\circ = \Delta G^{hemi} + RT \ln [HOH] + \Delta G^{HB}$

Pivot u: (1,0,0) → (0,1,1)

$H_2OH^+ + RCH_2O^- + H_2C{=}O + HB \rightarrow H_2O + RCH_2{\cdot}OH^+{\cdot}CH_2OH + B^-$

$\Delta G'_u = \Delta G^{HB} - RT \ln [HOH] - \Delta G^{IH} - \Delta G^{HOR} + \Delta G^{hemi}$
$\gamma = 18.49 \pm 0.11$; $\mu_u = 24.8 \pm 6.9$; $\mu'_u = 2.75 \pm 0.46$
σ(fit) = 0.153; σ(data) = 0.250 kcal

Pivot v: (0,1,0) → (1,0,1)

$H_2O + RCH_2{\cdot}OH^+{\cdot}CH_2O^- + HB \rightarrow H_2OH^+ + RCH_2O^- + H_2C{=}OH^+ + B^-$

$\Delta G'_v = \Delta G^{HB} + RT \ln [HOH] - \Delta G^Z + \Delta G^{HOR} - \Delta G^K - \Delta G^{hemi}$
$\gamma = 18.93 \pm 0.15$; $\mu_v = 13.4 \pm 1.7$; $\mu'_v = 269$
$1/\mu'_v = 0.0037 \pm 0.003$; σ(fit) = 0.138; σ(data) = 0.245 kcal

Pivot w: (0,0,1) → (1,1,0)

$H_2O + RCH_2OH + H_2C{=}OH^+ + B^- \rightarrow H_2OH^+ + RCH_2OCH_2O^- + HB$

$\Delta G'_w = -\Delta G^{HB} + RT \ln [HOH] + \Delta G^I + \Delta G^K + \Delta G^{hemi}$
$\gamma = 18.22 \pm 0.20$; $\mu_w = -6.4 \pm 2.0$; $\mu'_w = 10.8 \pm 1.1$
σ(fit) = 0.146; σ(data) = 0.250 kcal

[a] Numerical data are given in kcal. $\Delta G_r^* + RT \ln [HOH] = -RT \ln ({}^a k_r/[HOH]) + RT \ln (k_B T/h)$. [a] k_r is the rate constant reported by FAJ for the reverse reaction in (1). It is divided by [HOH] because in the forward reaction of mechanism 4, HOH is a reagent.

Transition-state coordinates (11) are derived from (10) by finding the coordinates where G is a maximum.

$$x^* = {}^1/_2 + \Delta G^\circ/8\gamma \tag{11a}$$

$$y^*_p = {}^1/_2 - \Delta G'_p/8\mu_p \tag{11b}$$

$$s^*_p = {}^1/_2 - \Delta G''_p/8\mu'_p \tag{11c}$$

Upon substituting in (10) we obtain the structure-energy relationship:

$$\Delta G^* = G[x^*,y^*,s^*] - G[0,{}^1/_2,{}^1/_2] = \gamma + {}^1/_2\Delta G^\circ + (\Delta G^\circ)^2/16\gamma - (\Delta G'_p)^2/16\mu_p - (\Delta G''_p)^2/16\mu'_p \tag{12}$$

Test of Mechanism (4). The basic equation is (12); specific equations are listed in Table II. The required free-energy quantities were taken from part 1.[1] Acid-catalyzed rate constants were taken from FAJ.[5] A 5 × 5 array of data was used, with the following substituents: R = CH_3, CH_3OCH_2, $ClCH_2$, Cl_2CH, and CF_3; R′ = H, $ClCH_2$, CH_3O, Cl, and CN. As in part 1, standard error estimates were 0.14 kcal for ΔG_+^* and 0.4 kcal each for ΔG°, $\Delta G'_p$, and $\Delta G''_p$.

The fit of the data to mechanism 4 can be tested by using either u, v, or w as pivot variable. Results of the least-squares fit for each pivot are included in Table II. The fits are good: σ(fit) is 0.14–0.15 kcal, well within the 0.25-kcal data error indicated by σ(data). Although the calculations with different pivots involve basically the same free-energy quantities, I believe that the fits are practically independent. The specific fitting equations are nonlinear and, as shown in Table I, utilize different combinations of $\Delta G'_u$, $\Delta G'_v$, and $\Delta G'_w$.

The test of mechanism 4 involves three adjustable parameters, while the previous tests of mechanism 2 and 3 involved only two. I therefore wish to show that the present test is significant and that the good fit is not merely due to the greater number of parameters. I shall show (a) that three-parameter equations for mechanisms with three progress variables are selective of mechanism, and (b) that in special cases involving three progress variables, equations with two parameters work well.

Concerning (a), an alternative, formally acid-catalyzed mechanism with three progress variables is shown below:

$$HB + HOH \overset{fast}{\rightleftharpoons} B^- + HOH_2^+ \tag{13a}$$

$$B^- + HOCH_2R + H_2C{=}O + HOH_2^+ \overset{k_+}{\rightleftharpoons} BH + RCH_2OCH_2OH + OH_2 \tag{13b}$$

The rate-determining step (13b) was treated by the same theory as above. Although three parameters were used, the fit was poor. The fitting procedure converged only for two out of three pivots, and at convergence σ(fit) was >0.4 kcal, while σ(data) was <0.25 kcal.

Concerning (b), the data in Table II show that when the pivot is v, μ'_v is relatively large so that the term $(\Delta G''_v)^2/16\mu'_v$ is relatively negligible. Accordingly, when the test for mechanism 4 was repeated using a two-parameter equation based on (12) but from which that term had been omitted, the fit remained quite good: σ(fit) = 0.153 kcal. The result shows that, given the right mechanism and an appropriate pivot, one can obtain good fit with only two parameters.

Granting that mechanism 4 fits the rate constants for acid catalysis, one may ask whether this conclusion introduces inconsistencies with other data. I shall address specifically two questions: (a) Why do the rate constants for *base* catalysis indicate a mechanism[1] without participation by water as a reagent? (b) Why does one not observe a kinetic term for cooperative catalysis by both buffer acid and buffer base?

In reaction 4, H_2O acts as proton acceptor and HB as proton donor. This mechanism belongs to a class called "push-pull" by Swain and co-workers.[8] The reaction thus may be written in more general form according to:

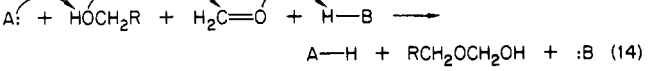

$$A{-}H + RCH_2OCH_2OH + :B \tag{14}$$

Corner species in the (u,v,w) progress cube for reaction 14 can be derived by simple inspection. For instance, (0,1,0) = A: + $RCH_2{\cdot}OH^+{\cdot}CH_2O^-$ + HB; (1,0,0) = A—H + RCH_2O^- + $H_2C{=}O$ + HB; etc. the theoretically required free-energy changes thus are readily derived. Moreover, since (4) and (14) belong to the same mechanistic family, their free-energy spaces are described by the same intrinsic constants. That is to say, the values of γ, μ_p, and μ'_p listed in Table II for reaction 4 apply also to any reaction according to (14). It is therefore possible to use eq 12, in conjunction with specific equations similar to those in Table II, to predict rate constants. I have used this technique (with v as pivot variable) to answer the questions posed above.

(a) Equation 14 predicts a kinetic term for general base catalysis if A: is identified with the general base, and HB and :B are taken to be HOH and OH^-, respectively. Rate constants for general base catalysis predicted in this way amount only to small fractions, 0.0003 to 0.034, of the observed rate constants. The dominant part of the base-catalyzed reaction thus is predicted to proceed

(8) (a) Swain, C. G.; Eddy, R. W. *J. Am. Chem. Soc.* **1948**, *70*, 2989. (b) Swain, C. G.; Brown, J. F. *Ibid.* **1952**, *74*, 2534, 2538, 2691. (c) Swain, C. G.; Kreevoy, M. M. *Ibid.* **1955**, *77*, 1122. (d) Swain, C. G.; Stivers, E. C.; Reuwer, J. F.; Schaad, L. J. *ibid.* **1978**, *80*, 5885.

Table III. Consistency of Predictions with Different Pivots

R[a]	R'[a]	pivot	u^*	v^*	w^*
CH_3	CN	u	0.383	0.803	0.343
		v	0.379	0.757	0.392
(17.866)[b]		w	0.412	0.862	0.254
		mean	0.391 ± 0.01	0.807 ± 0.03	0.330 ± 0.04
$ClCH_2$	CH_3O	u	0.435	0.779	0.349
		v	0.408	0.734	0.417
(19.078)[b]		w	0.448	0.795	0.319
		mean	0.430 ± 0.01	0.769 ± 0.02	0.361 ± 0.03
CF_3	H	u	0.493	0.749	0.354
		v	0.440	0.708	0.445
(20.506)[b]		w	0.488	0.720	0.388
		mean	0.474 ± 0.02	0.726 ± 0.01	0.396 ± 0.03

[a] Substituent in RCH_2OH or $R'CH_2COOH$, respectively. [b] ΔG_+^* (kcal).

by a mechanism other than that shown in (14). This is consistent with deductions made in part 1.[1] Although not assisted by proton transfer from HOH, the dominant base-catalyzed reaction is faster than (14) because its product, $RCH_2OCH_2O^-$, is a weaker base than OH^-. (See data for ΔG^I in part 1, Table I.) There is no inconsistency.

(b) In buffered solutions, eq 14 predicts a kinetic term in which HB represents the buffer acid and A: represents the conjugate buffer base B^-. The corresponding kinetic contribution to the reverse reaction ($RCH_2OCH_2OH \rightarrow RCH_2OH + H_2C{=}O$) is a third-order term, $k_{III}[RCH_2OCH_2OH][HB][B^-]$. Such kinetic terms are well known for the enolization of acetone.[9a] FAJ[5] looked for such a term for the present reaction but could not find it. To test whether the predicted third-order reaction would be fast enough to be detected, I calculated k_{III} for each member of the reaction series and multiplied it by the *maximum* product of relevant experimental concentrations to obtain the maximum third-order rates predicted according to (14). These maximum rates were always less than 20% of the total rates, and mostly less than 10%. Considering that the kinetic analysis[5] already involves five terms, an additional sixth term that amounts to less than 20% under all conditions probably cannot be detected. This is not because the experimental error is 20% (the actual error may be several times smaller) but because statistical covariance permits compensating changes to be made in the other fitted rate constants so that the third-order kinetic term may be omitted without appreciable deterioration of the fit. Again, there is no inconsistency.[9b] Thus, by the criteria of the present approach, eq 4 may, and indeed does, represent the dominant mechanism for the general acid catalyzed reaction.

Transition-State Coordinates. Values of x^*, y^*_p, and s^*_p [$p = u,v,w$] were calculated for reaction 4 from eq 11, and values of u^*, v^*, and w^* were calculated using equations given in Table I. Since the statistical fits with different pivots are nearly independent, agreement among the three sets of results would tend to confirm their validity. However, one must not be too finicky, for the following reason. The crux of the present theory is that any initial set of progress variables can be transformed, first into a set (u,v,w) and then into a set $[x,y,s]$, such that $G(x,y,s)$ is a quadratic function according to (10). If the transformed function fits only approximately rather than exactly, the error in ΔG^* will be small, because G is at a maximum and the free-energy hypersurface is stationary at the transition state. On the other hand, and for the same reason, errors in u^*, v^*, and w^* will be large.

In fact, the precision of results based on the three pivots is respectable. Representative results are shown in Table III. Standard deviations of mean results are: 0.015 for u^*, 0.03 for v^*, and 0.04 for w^*.

(9) (a) Albery, W. J.; Gelles, J. S. *J. Chem. Soc., Faraday Trans. 1* **1982**, *78*, 1569. (b) In FAJ's experiments, buffer concentrations ranged up to 0.5 M at a constant total ionic strength (KCl) of 1.0 M. One cannot safely increase the buffer concentration and thus increase the relative importance of the third-order term because specific medium effects then seriously perturb the kinetic analysis, even at constant ionic strength. Hand, E. S.; Jencks, W. P. *J. Am. Chem. Soc.* **1975**, *97*, 6221.

Table IV. Some Transition-State Coordinates (u^*, v^*, w^*)[a] for the Reaction Series

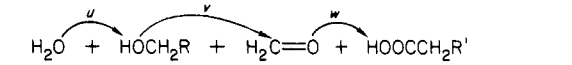

R' in acid (pK_a)	R in alcohol (pK_a)		
	CH_3 (16.0)	$ClCH_2$ (14.3)	CF_3 (12.4)
H (4.7)	0.40, 0.88, 0.32	0.44, 0.80, 0.36	0.47, 0.73, 0.40
CH_3O (3.4)	0.40, 0.84, 0.32	0.43, 0.77, 0.36	0.47, 0.69, 0.40
CN (2.2)	0.39, 0.81, 0.33	0.43, 0.74, 0.37	0.46, 0.66, 0.41

[a] Mean values for three pivots. Standard deviations of the mean are 0.015 for u^*, 0.03 for v^*, and 0.04 for w^*.

Table IV lists mean results for a representative array of substituents. Although the variability of (u^*,v^*,w^*) for the acid-catalyzed reaction is much less than that of (u^*,v^*) for the base-catalyzed reaction (part 1, Table III),[1] the tabulated changes are significant. All three progress variables depend noticeably on the pK_a of the alcohol; the directions of change agree with expectation. The progress of C···O bond formation (v^*) is also quite sensitive to changes in the pK_a of the acid catalyst, while u^* and w^* are comparatively insensitive. Throughout Table IV, v^* is well ahead of u^* and w^*; that is, C···O bond formation at the transition state is well ahead of the proton transfers.

Critique of Theory. Point of Maximum Disparity. It is encouraging that reaction mechanisms can be identified so decisively and consistently by the present methods. The validity of the results depends, of course, on the validity of the basic theory. In this and the following section I shall consider two of the physical assumptions.

One of the assumptions is to use the relatively simple eq 10, which contains no cross terms of progress variables, rather than the more general quadric eq 15. (The subscripts indicating the pivot variable have been omitted.) When two progress variables are sufficient, eq 15 reduces to the previously discussed[2] eq 16.

$$G = c + 4\gamma x(1-x) + \Delta G^\circ x - 4\mu y(1-y) + \Delta G' y - 4\mu' s(1-s) + \Delta G'' s \quad (10)$$

$$G = c + 4\gamma x(1-x) + \Delta G^\circ x - 4\mu y(1-y) + \Delta G' y + f(x-\tfrac{1}{2})(y-\tfrac{1}{2}) - 4\mu' s(1-s) + \Delta G'' s + g(x-\tfrac{1}{2})(s-\tfrac{1}{2}) + h(y-\tfrac{1}{2})(s-\tfrac{1}{2}) \quad (15)$$

$$G = c + 4\gamma x(1-x) + \Delta G^\circ x - 4\mu y(1-y) + \Delta G' y + f(x-\tfrac{1}{2})(y-\tfrac{1}{2}) \quad (16)$$

The cross term in (16) vanishes when the reaction series may include identity reactions,[2] for reasons of symmetry. However, many reaction series (including addition reactions to a carbonyl group) have transition states that are inherently unsymmetrical, and symmetry arguments cannot be applied. Since even for such reactions the cross term does not seem to be needed, I wish to derive an alternative, symmetry-independent condition for the absence of cross terms.

Using eq 16, let us consider the slope of the reaction coordinate z at the transition state. The reaction coordinate is specified when either the y coordinate y_z is known as a function of x, or when x_z is known as a function of y. The derivative, dy_z/dx, denotes the slope of the reaction coordinate with respect to the x axis.

Jencks and Jencks[10] have described an elegant method for obtaining dy_z/dx at the transition state (TS) on free-energy surfaces of the general form of eq 16. As expected, $(dy_z/dx)_{TS}$ is a function of f. Furthermore, when $f = 0$, $(dy_z/dx)_{TS} = 0$. That is to say, when $f = 0$ the reaction coordinate runs parallel to the x axis at the transition state and, more important, y_z goes through an extremum. (The possibility that y_z as a function of x has an inflection point at the transition state may be ruled out because the free-energy surface is quadratic.) An extremum in y_z implies that the disparity of progress of the reaction events ($v - u$) attains

(10) Jencks, D. A.; Jencks, W. P. *J. Am. Chem. Soc.* **1977**, *99*, 7948. dy_z/dx was calculated from the slopes of the level lines passing through the free-energy point of the transition state. See eq 15 and 16 of ref 10.

its maximum magnitude at the transition state. Thus, in cases with two progress variables, omitting the pairwise cross term is equivalent to requiring that disparity of progress reaches a maximum at the transition state.

I believe this is a physically plausible constraint. The freedom of two reaction events to progress with disparity lowers the free energy below what it otherwise would be.[2] This lowering, and the disparity which causes it, may well be greatest at the point of highest free energy, the transition state.

In case of eq 15, on applying the method of Jencks and Jencks[10] one finds: (a) $f = 0$ implies that $(\partial y_z/\partial x)_{s,TS} = 0$; (b) $g = 0$ implies that $(\partial s_z/\partial x)_{y,TS} = 0$. Together these conditions constrain the reaction coordinate from reagents to products to run parallel to the x axis at the transition state. The further condition that $h = 0$ additionally constrains the reaction coordinate for the disparity reaction along y, $[^1/_2,0,^1/_2] \rightarrow [^1/_2,1,^1/_2]$, to run parallel to the y axis at the transition state.

Constancy of Intrinsic Parameters. The present theory allows for progress of the concerted reaction events to vary with the individual reaction but treats the intrinsic parameters (γ, μ, μ') as constants of the reaction family. This introduces error if these parameters, in fact, vary with the reaction, especially when the variable parameter is γ.

The intrinsic parameters remain constant *by definition* if the substituents are introduced in the molecule at sites that are well removed and electronically insulated from the reaction zone. According to Thornton's model,[11] the substituent effects may then be treated as linear perturbations of an otherwise unchanged free-energy surface whose parameters (γ, μ, μ') are constants of the reaction family. Since this is the model actually used, substituents were chosen accordingly. All substituents included in the present study are external to the reaction zone and separated from the nearest reaction site by at least one CH_2 group.

Real substituents that cause measurable effects on $\Delta G^{\ddagger}$ do not conform rigorously to the idealized model. It is therefore of interest to consider the sensitivity of γ to likely interactions. In particular, one would like to define the constraints that must be imposed in order for γ to remain constant.

In a recent series of papers on displacement reactions at a carbon atom, Shaik and Pross[12] described an interaction mechanism which, in the present terminology, causes the force constant of the reactant bond to vary within a reaction series. Although Shaik and Pross considered a specific mechanism, the possibility that the force constant may change is general. I wish to consider the effect on γ and derive conditions under which the change in γ will be small.

When disparity of concerted reaction events is neglected, γ is equal to $\Delta G^{\ddagger}$ for reactions in which $\Delta G^{\circ} = 0$. Accordingly, I shall consider a series of identity reactions in which the force constant of the reactant bond is variable and inquire whether $\Delta G^{\ddagger}$ can remain constant. The necessary condition is shown in Figure 5; $\Delta G^{\ddagger}$ and thus γ will remain constant if the change in the force constant k is accompanied by an appropriate change in the bond stretching ($r^{\ddagger} - r_e$) at the transition state, expressed in (17), where r_e denotes the equilibrium bond distance of the reactant bond.

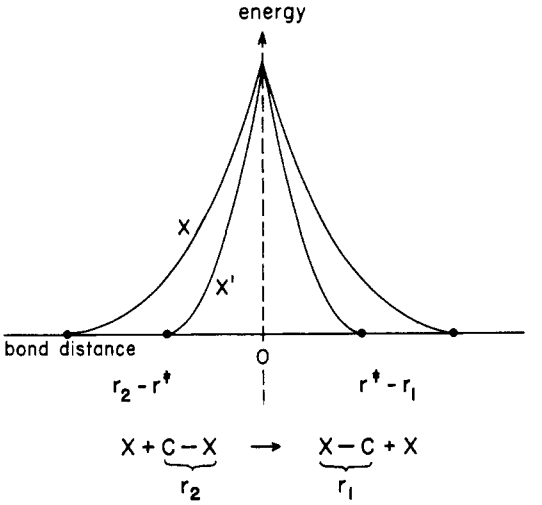

Figure 5. Bond stretching at the transition state as a function of force constant when the intrinsic barrier γ is constant.

$$\gamma = \tfrac{1}{2}k(r^{\ddagger} - r_e)^2 = \text{constant} \qquad (17)$$

A classical relationship between k and r_e is given in (18), in which

$$k = Ar_e^{-n} \qquad (18)$$

$$(r^{\ddagger} - r_e)/r_e = (\text{const})r_e^{(n-2)/2} \qquad (19)$$

the parameter n is typically in the range 4 6.[13] 6.[13] Substitution in (17) then leads to (19), which expresses the mathematical condition for γ to be a constant of the reaction series. Since the exponent, $(n - 2)/2$, in (19) is in the range 1 to 2, eq 19 requires that the fractional bond stretching at the transition state must increase with the equilibrium distance of the reactant bond. This is a plausible possibility. It will be of interest to inquire if and when it can really happen.

Registry No. $NCCH_2COOH$, 372-09-8; $ClCH_2COOH$, 79-11-8; CH_3OCH_2COOH, 625-45-6; $ClCH_2CH_2COOH$, 107-94-8; CH_3COOH, 64-19-7; CF_3CH_2OH, 75-89-8; Cl_2CHCH_2OH, 598-38-9; $ClCH_2CH_2OH$, 107-07-3; $CH_3OCH_2CH_2OH$, 109-86-4; CH_3CH_2OH, 64-17-5; HCHO, 50-00-0.

(11) Thornton, E. R. *J. Am. Chem. Soc.* **1967**, *89*, 2915.
(12) Pross, A.; Shaik, S. S. *Acc. Chem. Res.* **1983**, *16*, 363.
(13) Morse, P. M. *Phys. Rev.* **1929**, *34*, 57.